UHPLC-Q-Orbitrap HRMS-Based Metabolomic Show Biological Pathways Involved in Rice (*Oryza sativa* L.) under Fe Toxicity Stress

(Metabolomik UHPLC-Q-Orbitrap Berasaskan HRMS menunjukkan Laluan Biologi Terlibat untuk Beras (*Oryza sativa* L.) di bawah Tekanan Ketoksikan Fe)

TURHADI TURHADI[1,2], HAMIM HAMIM[3], MUNIF GHULAMAHDI[4] & MIFTAHUDIN MIFTAHUDIN[3,*]

[1]*Plant Biology Graduate Program, Department of Biology, Faculty of Mathematics and Natural Sciences, IPB University, Kampus IPB Dramaga 16680 Bogor, West Java, Indonesia*
[2]*Department of Biology, Faculty of Mathematics and Natural Sciences, Universitas Brawijaya, Jl. Veteran, Malang 65415, East Java, Indonesia*
[3]*Department of Biology, Faculty of Mathematics and Natural Sciences, IPB University, Kampus IPB Dramaga 16680 Bogor, West Java, Indonesia*
[4]*Department of Agronomy and Horticulture, Faculty of Agriculture, IPB University, Kampus IPB Dramaga 16680 Bogor, West Java, Indonesia*

ABSTRACT

The iron (Fe) toxicity stress is still a serious problem in rice cultivation, especially on land with high Fe content. The Fe toxicity stress affects various complex physiological aspects of plants. The metabolomic analysis using LC-MS is expected to provide information about rice's metabolism regulation under Fe toxicity stress. The objective of this study was to show the biological pathway signature in rice after exposure to Fe toxicity stress using UHPLC-Q-Orbitrap HRMS-based metabolomic analysis. The two rice varieties, i.e., IR64 (Fe-sensitive) and Pokkali (Fe-tolerant) were analyzed their metabolites using UHPLC-Q-Orbitrap HRMS. The metabolite profiles of both varieties were analyzed using MetaboAnalyst 5.0 software. The results showed that Fe toxicity stress affected the metabolite profile in both root and shoot tissues of two rice varieties. A number of 102 metabolites were detected in root and shoot tissues of rice. The comprehensive univariate and multivariate analyses showed that 1-aminocyclopropane-1-carboxylate (ACC) in shoot tissues and galactose in root tissues was suggested as metabolite markers for Fe tolerance character of rice var. Pokkali. The genes encoded the enzymes involved in biosynthetic pathway of both metabolite markers could be a target to be explored for Fe toxicity tolerance in rice.

Keywords: Galactose; metabolism; metabolite markers; 1-aminocyclopropane-1-carboxylate

ABSTRAK

Tekanan ketoksikan besi (Fe) masih menjadi masalah serius dalam penanaman padi, terutamanya pada tanah yang mempunyai kandungan Fe yang tinggi. Tekanan ketoksikan Fe mempengaruhi pelbagai aspek fisiologi tumbuhan yang kompleks. Analisis metabolomik menggunakan LC-MS dijangka memberikan maklumat tentang peraturan metabolisme beras di bawah tekanan ketoksikan Fe. Objektif kajian ini adalah untuk menunjukkan pengenalan laluan biologi dalam beras selepas terdedah kepada tekanan ketoksikan Fe menggunakan analisis metabolomik berasaskan UHPLC-Q-Orbitrap HRMS. Kedua-dua varieti beras, iaitu IR64 (Fe-sensitif) dan Pokkali (Fe-toleransi) telah dianalisis metabolitnya menggunakan UHPLC-Q-Orbitrap HRMS. Profil metabolit kedua-dua jenis varieti dianalisis menggunakan perisian MetaboAnalyst 5.0. Keputusan menunjukkan bahawa tekanan ketoksikan Fe mempengaruhi profil metabolit dalam kedua-dua tisu akar dan pucuk kedua-dua varieti padi. Sejumlah 102 metabolit telah dikesan dalam tisu akar dan pucuk padi. Analisis komprehensif univariat dan multivariat menunjukkan bahawa 1-aminosiklopropana-1-karboksilat (ACC) dalam tisu pucuk dan galaktosa dalam tisu akar telah dicadangkan sebagai penanda metabolit untuk sifat toleransi Fe bagi beras var. Pokkali. Gen yang mengekod enzim yang terlibat dalam laluan biosintetik kedua-dua penanda metabolit boleh menjadi sasaran untuk diterokai untuk toleransi ketoksikan Fe dalam beras.

Kata kunci: Galaktosa; metabolisme; penanda metabolit; 1-aminosiklopropana-1-karboksilat

INTRODUCTION

Interaction of various metabolites related to metabolic processes are needed for the survival of an organism. As a sessile organism, plants have various mechanisms to withstand unfavorable conditions, both biotic and abiotic stresses. Metabolite compounds that the plant produces represent their genetic background (Hill & Roessner 2013). The metabolite concentration depends on the genetic background and their surrounding environment (Hall & Hardy 2012).

The Fe toxicity stress is known as a serious problem for crops. The complex impacts due to Fe toxicity stress in plants and their tolerance strategy have been studied previously (Audebert & Sahrawat 2000; De Dorlodot, Lutts & Bertin 2005; Engel, Asch & Becker 2012; Kabir et al. 2016; Wu et al. 2016, 2014). The Fe toxicity stress is known to impair the metabolic balance, and consequently inhibit rice growth and development (Aung & Masuda 2020; Aung et al. 2018; Mahender et al. 2019; Stein et al. 2019). Fe toxicity has also been reported to reduce the morpho-physiological characters of several plants, such as corn (Kovačević, Vukadinović & Bertić 1988), British native fen plant species (*Eriophorum angustifolium*, *Carex lepidocarpa*, *Lotus uliginosus*, *Lychnis flos-cuculi*) (Snowden & Wheeler 1993), *Tagetes erecta* (Albano, Miller & Halbrooks 1996), *Glyceria fluitans grass* (Lucassen, Smolders & Roelofs 2000), and hexaploid wheat (Khabaz-saberi et al. 2010). To the best of our knowledge, there were few references reported the global metabolite snapshot related to Fe toxicity stress in plants. Turhadi et al. (2019) reported that linoleic- and linolenic acid are metabolite markers for rice response to Fe toxicity stress based on GC-MS-based metabolomic study. Those linoleic- and linolenic acid might maintain the membrane fluidity and permeability during Fe toxicity stress.

As a final product of gene expression, metabolite compounds are considered to describe the biochemical conditions of an organism due to external stimuli (Jorge et al. 2016). Fe toxicity stress is known to affect the various gene and protein activities. The activity of genes and proteins are needed for the mechanism of homeostasis, transport, and survival during Fe toxicity stress conditions (Bashir et al. 2014; do Amaral et al. 2016; Finatto et al. 2015; Quinet et al. 2012). Finally, this regulation affects the metabolism of rice. The metabolomic approaches offers a more comprehensive analysis of the metabolite profile when the plant metabolism changes under certain conditions (Gupta & De 2017; Turhadi et al. 2019; Wang et al. 2015; Widodo et al. 2009).

Various strategies in the metabolomic analysis are used to detect and measure the presence of metabolites, for example, Liquid Chromatography-Mass Spectrophotometry (LC-MS). The metabolite profiling via LC-MS was carried out in the liquid phase and a wide range of detection abilities (Obata & Fernie 2012). According to Sangwan et al. (2015), LC-MS could also detect the plant secondary metabolite groups. Kusano et al. (2015) reported that more than 1000 metabolites compounds were found in rice. Some of these metabolite compounds play a role in dealing with biotic and abiotic stresses. This study aimed to show the biological pathway signature in rice after exposure to Fe toxicity stress using UHPLC-Q-Orbitrap HRMS-based metabolomic analysis. The results of the study are expected to provide information about tolerance mechanism of rice to Fe toxicity stress. Furthermore, the results also provide information for further studies, especially for molecular aspects regarding genes involved in metabolite marker biosynthesis.

MATERIALS AND METHODS

PLANT MATERIALS AND EXPERIMENTAL DESIGN

Two-weeks-old of rice var. IR64 (Fe-toxicity sensitive) and var. Pokkali (Fe-toxicity tolerant) were used in this experiment (Turhadi et al. 2018). Growth of plants were conducted on half-strength of a hydroponic system using Yoshida's solution (Yoshida et al. 1976) with 0.2% agar addition (Figure 1) (Nugraha et al. 2015; Turhadi et al. 2021). There were two kinds of Fe treatments added on a hydroponic solution, namely 0 ppm (control) and 400 ppm (Fe-toxic) in the form of $FeSO_4 \cdot 7H_2O$. The treatments were performed for ten days using a complete randomized design with three replications. The samples were harvested ten days after treatment for metabolite extraction.

SAMPLE PREPARATION AND UHPLC-Q-ORBITRAP HRMS ANALYSIS

The samples were ground into fine powder using liquid nitrogen. The fine powder samples were extracted on ethanol pro-analyze (1 gram sample: 10 mL solvent). The extracted samples were then analyzed using *Vanquish Flex UHPLC Tandem Q Exactive Plus Orbitrap-High Resolution Mass Spectrophotometry* (*Thermo Scientific, Germany*). The analysis used *Accucore™ Phenyl-Hexyl LC Columns*, 2.1 mm × 100 mm; 2.6 μm (*Thermo Scientific, Germany*) column. The mobile phase comprised of methanol (LC-MS grade) (mobile phase A) and 0.1%

FeTox = Fe toxicity stress treatment

FIGURE 1. The experimental setting for hydroponic condition in this research

formic acid in water (mobile phase B). The flow rate of 0.2 mL/min and inject a volume of 5 µL were used in this study. The program was set to 98% A (0-1 min), 98-60% A (1-5 min), 60-30% A (5-12 min), 30-5% (12-25 min). The column was set at 40 °C during analysis. Positive and negative ionization in the range of 80-1000 m/z were used in this study.

FEATURE FINDING

Feature finding in mass spectra files were performed on MZmine 2.53 software. According to Oh et al. (2021), feature finding data follows mass detection, chromatogram builder, chromatogram deconvolution, isotoping, and alignment. Mass detection was set using wavelet transform mass detector algorithm with noise level cut-off at 1500 for MS1. The chromatogram was built with the minimum highest intensity of 5000, group intensity threshold of 0.01 min, and the m/z tolerance

at 0.001 m/z or 5 ppm. A baseline cut-off algorithm with a minimum peak height of 2500, peak duration range of 0.02-0.4 min, and baseline level were used in chromatogram deconvolution. The deconvoluted peaks were isotoped using isotopic peaks grouper with m/z tolerance of 0.006 m/z or 10 ppm, retention time tolerance 0.15 min, and a maximum charge of 1. These isotoped peaks were aligned using a join aligner module with an m/z tolerance of 0.006 min or 10 ppm, an absolute retention time tolerance of 0.3 min, an m/z weight, and a retention time weight of 70 and 30. The identified features in the blank injection sample, duplicated peaks, and features with less than three in a row in aligned peaks were manually removed.

An m/z tolerance of 0.5 m/z or 10 ppm with retention time tolerance of 0.1 min was used in metabolite identification. The metabolites were identified using an in-house database and published references (Begum et

al. 2016; Chang et al. 2012; Dong et al. 2014; Hu et al. 2016, 2014; Jung et al. 2013; Lim et al. 2018a, 2018b; Navarro-Reig et al. 2017, 2015; Xiao et al. 2018).

STATISTICAL DATA ANALYSIS

Univariate and multivariate analyses were performed using MetaboAnalyst 5.0 (http://www.metaboanalyst. ca) (Xia & Wishart 2016). In order to show the distribution of annotated metabolites, scatter plots were performed using R-studio. Fold change analysis and Student's T-test were performed to elucidate the effect of treatment on metabolites with α=0.05. A mean-centered normalization was subjected to the metabolite dataset before performing the principal component analysis (PCA), Partial Least Square-Discriminant Analysis (PLS-DA), and heatmap clustering analysis (HCA). The PLS-DA model is validated using several parameters, i.e., predictive capability of model (Q^2), correlation coefficient of model (R^2), model reproducibility (Q^2/R^2),

and the value in component based on the best classifier of Q^2 value to classify the sample using leave-one-out cross-validation (LOOCV) (data not shown). Euclidean's distance and Ward's hierarchical clustering algorithm were used in the HCA. The pathway analysis was performed to identify the affected metabolic pathways based on the KEGG pathway for *Oryza sativa*.

RESULTS

COMPARISON OF METABOLITE DIVERSITY IN RICE BETWEEN CONTROL AND FE TOXICITY STRESS CONDITION

A total of 102 metabolites were identified in rice using UHPLC-Q-Orbitrap HRMS. Most of them were primary metabolites, including amino acids and amino acid-related, carbohydrates and lipids, cofactors, nucleotides, organic acids, and other compounds with varied molecular weight and retention time (Figure 2(A)-2(B);
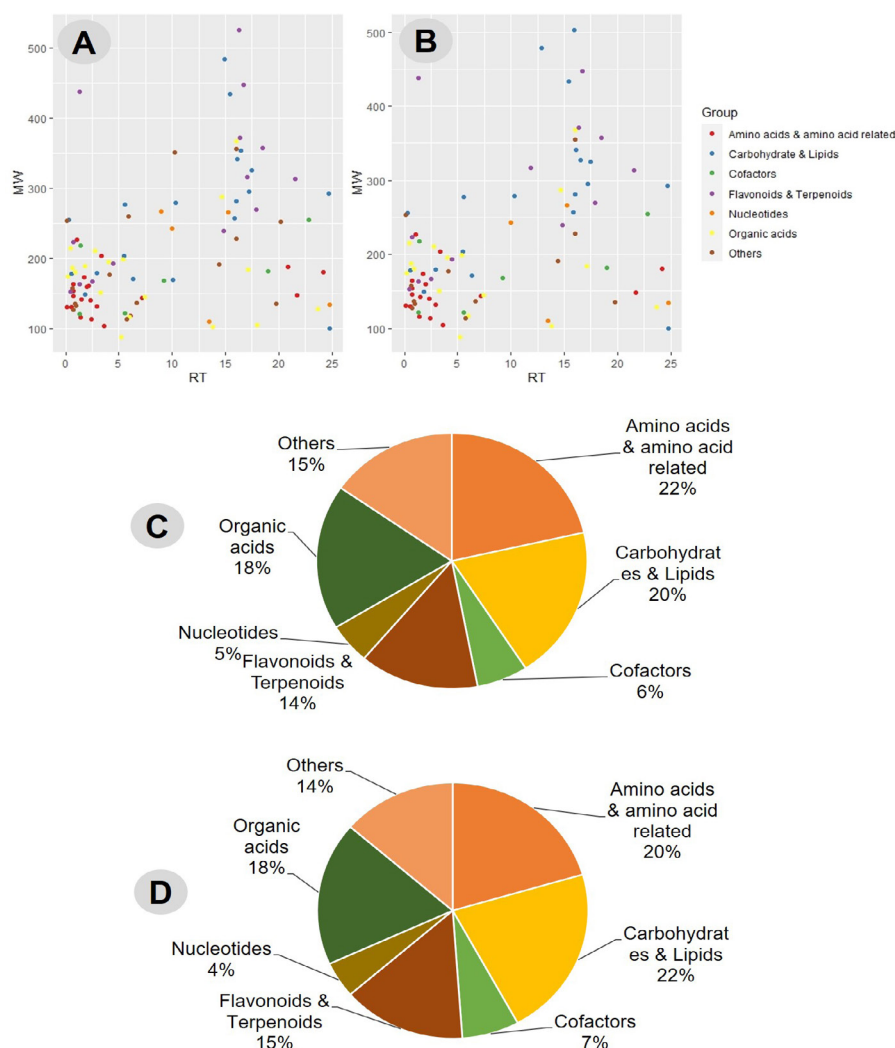
MW = molecular weight (g/mol); RT = retention time (min)

FIGURE 2. The comparison of detected metabolites composition in the shoot (A and C) and root (B and D) rice tissues in control and Fe toxicity stress condition

Supplementary Table S1). A total of 21 amino acids and amino acid-related, 19 carbohydrates and lipids, and 18 organic acids were identified as the top three of identified metabolites in shoot tissues (Figure 2(A)-2(C); Supplementary Table S1). Whereas, a total of 18 amino acids and amino acids related 19 carbohydrates and lipids and 16 organic acids were also identified as the top three of identified metabolites in root tissues (Figure 2(B)-2(D); Supplementary Table S1). Primary metabolites and secondary metabolites were identified in shoot and root tissues of rice using UHPLC-Q-Orbitrap HRMS.

A total of 14 and 13 secondary metabolites were also identified in shoot and root tissues (Figure 2(A)-2(D); Supplementary Table S1). Flavonoids and terpenoids groups were mainly identified in this study. These results suggested that a metabolomic study using UHPLC-Q-Orbitrap HRMS could detect both primary and secondary metabolites in rice after with and without Fe toxicity stress treatment. Table 1 shows the metabolite composition of the shoot and root tissues in two rice varieties with different tolerance levels to Fe toxicity stress, IR64 and Pokkali.

Principal component analysis (PCA) confirmed that the tissues (shoot and root) differ in their metabolite composition. The PC1 and PC2 showed that 54.2% in total variation cumulative (PC1, 30.7%; PC2, 23.5%) (Figure 3). This result was also supported by using clustering analysis (Figure 4(A)), which differed between shoot- and root tissues based on their metabolite composition. These results indicated that rice varieties, Fe toxicity treatment, and tissue types significantly impacted rice metabolite profiles. The difference of tissue performed the most obvious effect. Diversity of metabolite compositions accounted for that clear cluster separation (Figure 4(A)-4(J)). Using heatmap visualization, the profile of metabolite abundance in each group could identify. These results suggested that mostly metabolite of the shoot and root tissues in IR64 or Pokkali after exposure to Fe toxicity stress treatment. Both high- and low levels of metabolites regulated when those plants under Fe toxicity stress condition.
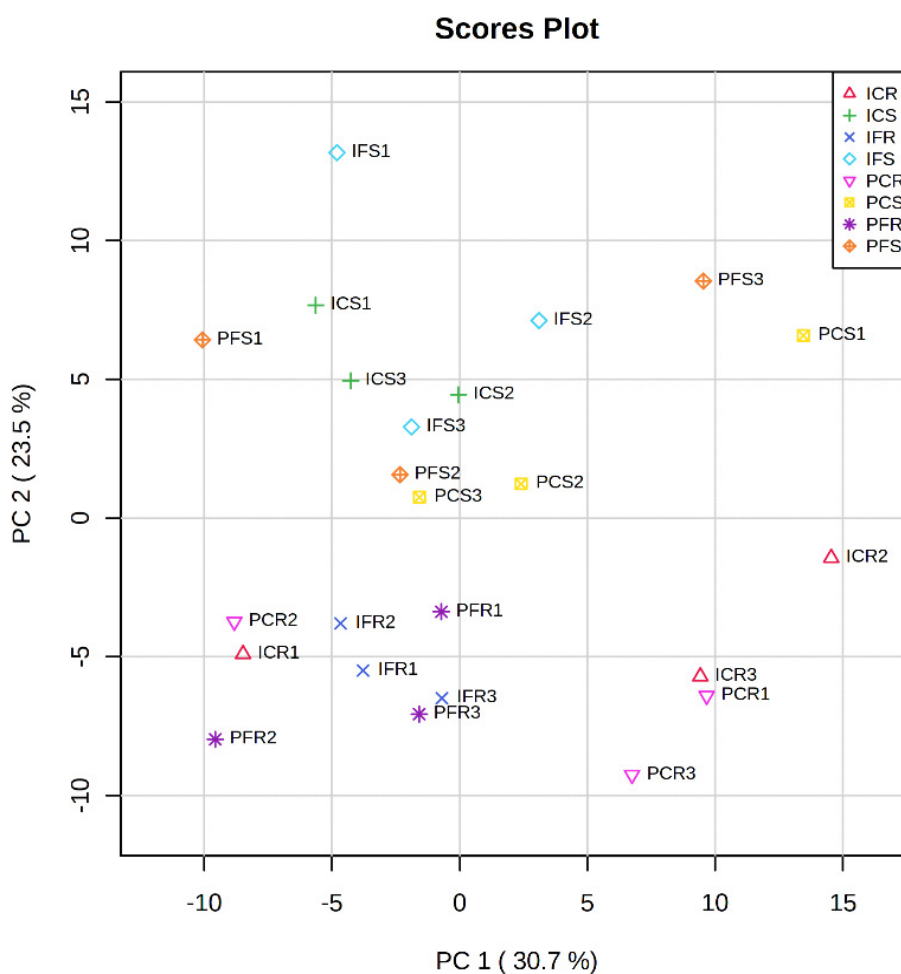
ICR = root of IR64 in control condition; ICS = shoot of IR64 in control condition; IFR = root of IR64 in Fe toxicity condition; IFS = shoot of IR64 in Fe toxicity condition; PCR = root of Pokkali in control condition; PCS = shoot of Pokkali in control condition; PFR = root of Pokkali in Fe toxicity condition; PFS = shoot of Pokkali in Fe toxicity condition. 1-3 = replications

FIGURE 3. Analysis of rice in control and Fe toxicity stress based on their metabolite composition using principal component analysis (PCA) plot
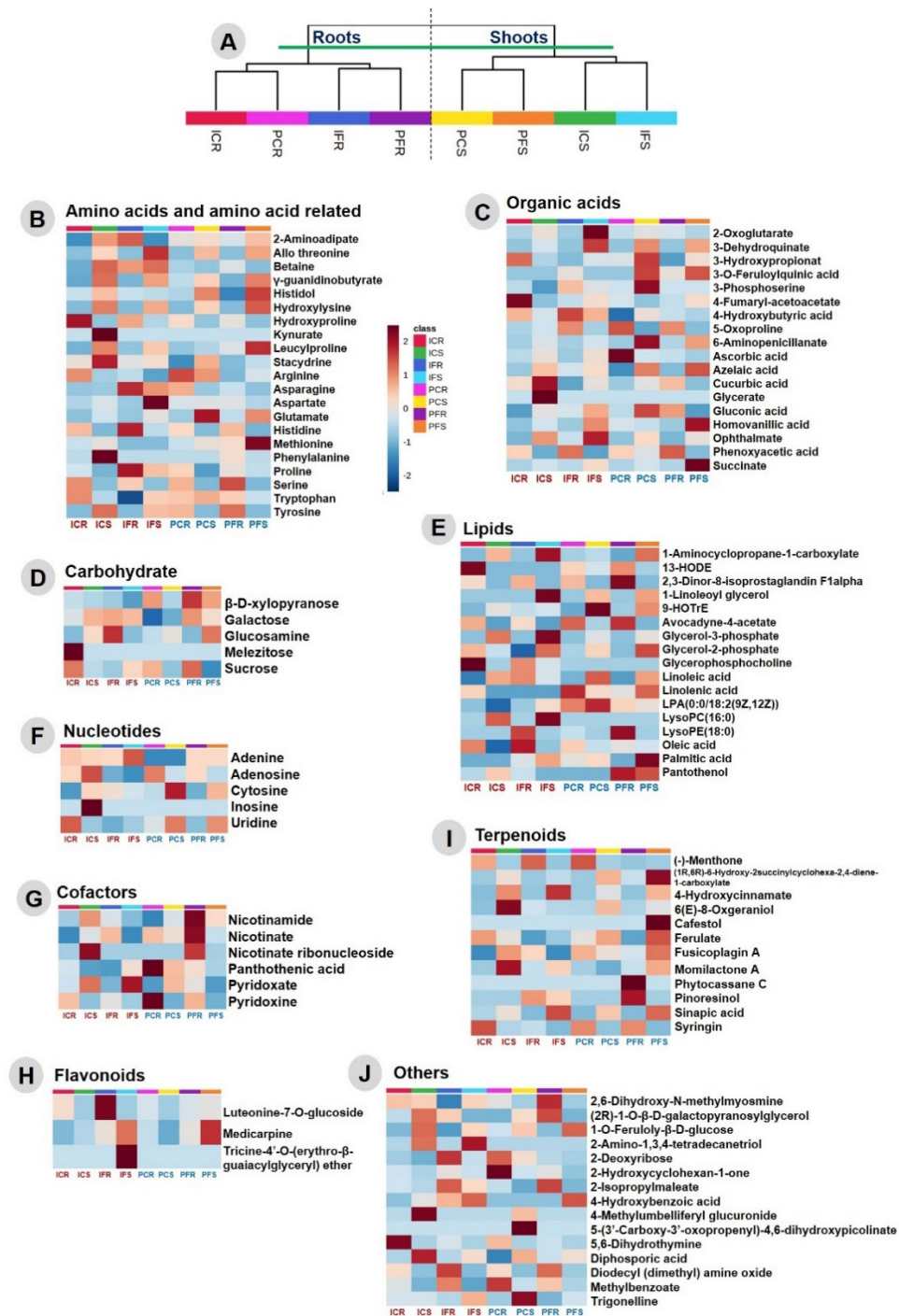
ICR = root of IR64 in control condition; ICS = shoot of IR64 in control condition; IFR = root of IR64 in Fe toxicity condition; IFS = shoot of IR64 in Fe toxicity condition; PCR = root of Pokkali in control condition; PCS = shoot of Pokkali in control condition; PFR = root of Pokkali in Fe toxicity condition; PFS = shoot of Pokkali in Fe toxicity condition

FIGURE 4. Analysis of rice in control and Fe toxicity stress based on their metabolite composition using clustering (A) and heatmap analysis (B-H)

IDENTIFICATION OF METABOLITE MARKERS AND ITS CORRESPONDING METABOLIC PATHWAY UNDER Fe TOXICITY STRESS CONDITION IN RICE

In shoot tissues of IR64 were identified ten metabolites significantly affected by Fe toxicity stress including four down- (cucurbic acid, panthothenol, 6(E)-8-Oxogeraniol, and Fusicoplagin A) and six up-accumulated (asparagine, aspartate, hydroxyproline, 3-dehydroquinate, 1-linoleoyl glycerol, and palmitic acid) (Table 1). Whereas, in the shoot of Pokkali were identified two up-accumulated metabolites (homovanillic acid and 1-aminocyclopropane-1-carboxylate (ACC)) under Fe toxicity stress (Table 1). Interestingly, these results also showed that under Fe toxicity stress, mostly primary metabolites in shoot tissues were significantly up-accumulated in both IR64 and Pokkali.

A total of eight and three metabolites were identified significantly regulated in the root of IR64 and Pokkali, respectively. Six metabolites up-accumulated (betaine, gluconic acid, succinate, linoleic acid, fusicoplagin A, and pinoresinol) and two metabolites down-accumulated (uridine and 5,6-dihydroxythymine) were identified in the root of IR64 (Table 1). At the same time, three metabolites up-accumulated (glutamate, gluconic acid, and galactose) were identified in the shoot of Pokkali (Table 1). Similar regulations were noted in metabolite of root when compared with shoot tissues. After exposure to Fe toxicity stress, primary metabolites in root tissues also were significantly up-accumulated in both IR64 and Pokkali.

TABLE 1. Fold changes (FC) and VIP score of identified metabolites in shoot and root tissues of rice var. IR64 and Pokkali after Fe toxicity stress treatment

Metabolite name	FC[a]				VIP scores[b]			
	Shoot		Root		Shoot		Root	
	IR64	Pokkali	IR64	Pokkali	IR64	Pokkali	IR64	Pokkali
Amino acids & related amino acids								
2-Aminoadipate	-4.37	1.19	8.67	-1.13	0.17	0.03	0.19	0.01
Allo-threonine	1.89	1.12	-1.26	-1.18	0.29	0.05	0.27	0.32
Arginine	-1.29	-1.37	-1.46	-2.10	0.10	0.23	0.20	0.39
Asparagine	2.63*	-1.11	3.65	-1.71	0.39	0.03	0.51	0.20
Aspartate	3.12*	-1.53	-1.34	1.10	1.01	0.18	0.06	0.04
Betaine	-1.02	-1.11	5.07*	1.49	0.02	0.04	0.82	0.20
γ-guanidinobutyrate	-1.17	1.36	1.28	-2.04	0.16	0.31	0.04	0.19
Glutamate	1.31	-1.39	1.34	1.85*	0.12	0.47	0.03	0.12
Histidine	2.41	-1.34	1.73	-1.32	0.43	0.09	0.96	0.02
Histidinol	-1.25	1.10	-1.01	-1.76	0.03	0.02	0.00	0.30
Hydroxylysine	-1.20	1.66	na[c]	na	0.25	0.74	na	na
Hydroxyproline	3.47*	-1.36	-1.70	-1.15	0.30	0.04	1.06	0.14
Kynurenate	-11.03	na	na	na	1.22	na	na	na
Leucylproline	-1.29	3.29	1.36	1.93	0.47	2.03	0.12	0.44
Methionine	-4.50	2.95	-5.33	1.71	0.10	0.28	0.06	0.05
Phenylalanine	-3.96	na	na	4.04	0.69	na	na	0.14
Proline	2.25	1.88	2.18	-1.14	0.15	0.09	0.18	0.02
Serine	1.06	-1.00	-1.27	1.33	0.01	0.00	0.14	0.20
Stacydrine	-1.66	-1.65	-1.07	1.64	0.26	0.21	0.02	0.07
Tryptophan	1.18	-1.21	-2.06	-1.00	0.04	0.05	0.12	0.00
Tyrosine	-1.37	na	na	1.34	0.04	na	na	0.03
Organic acids								
3-Dehydroquinate	3.32*	-1.11	na	na	0.26	0.03	na	na
3-Hydroxypropionate	1.16	-1.49	-2.15	-1.69	1.22	5.43	6.12	3.14
3-O-Feruloylquinic acid	na	-1.06	4.73	4.73	na	0.02	0.07	0.07
3-Phosphoserine	4.10	-2.98	1.94	-1.00	0.16	0.40	0.13	0.00
4-Fumaryl-acetoacetate	3.67	3.45	-3.92	-1.19	1.58	1.71	3.49	0.23

Metabolite name	FC[a]				VIP scores[b]			
	Shoot		Root		Shoot		Root	
	IR64	Pokkali	IR64	Pokkali	IR64	Pokkali	IR64	Pokkali
4-Hydroxybutyric acid	1.49	-1.44	1.35	3.80	0.52	0.41	0.46	0.64
2-Oxoglutarate	3.18	-1.97	-1.45	1.25	1.62	0.36	0.08	0.10
5-Oxoproline	-1.34	1.48	2.44	-1.18	0.09	0.07	0.31	0.09
6-Aminopenicillanate	-1.13	-1.70	1.13	2.38	0.04	0.76	0.01	0.08
Ascorbic acid	1.08	-1.61	-1.37	-3.65	0.02	0.10	0.04	0.50
Azelaic acid	-1.08	1.11	1.44	1.86	0.07	0.15	0.18	0.16
Cucurbic acid	-2.37*	-2.23	-4.96	2.57	1.78	0.77	0.97	0.93
Glycerate	-6.00	na	na	na	0.15	na	na	na
Gluconic acid	1.53	-6.52	5.45*	2.28*	0.07	0.26	0.08	0.10
Homovanillic acid	2.14	3.14*	1.18	na	0.87	1.71	0.06	na
Ophthalmate	1.46	-1.22	22.27	-4.44	0.71	0.19	0.38	0.09
Phenoxyacetic acid	-1.29	-2.08	1.44	1.39	0.06	0.42	0.35	0.35
Succinate	1.53	4.35	1.27*	1.07	0.35	2.51	0.08	0.02
Carbohydrate and Lipids								
β-D-xylopyranose	-1.48	1.66	-1.16	1.15	0.20	0.44	0.08	0.14
Galactose	-1.02	1.77	1.29	4.55*	0.02	0.37	0.18	0.65
Glucosamine	-2.02	1.58	3.74	-1.51	0.28	0.34	0.59	0.11
Melezitose	na	na	-3.92	na	na	na	0.19	na
Sucrose	1.20	-1.24	-1.54	1.13	1.10	1.01	2.27	0.77
1-Aminocyclopropane-1-carboxylate	1.69	2.33*	1.15	-2.02	2.79	3.24	0.16	0.75
1-Linoleoyl glycerol	6.74*	1.16	na	na	0.53	0.05	na	na
2,3-Dinor-8-isoprostaglandin F1alpha	na	na	1.33	1.85	na	na	0.03	0.11
13-HODE	na	-2.17	-4.35	1.49	na	0.16	0.81	0.20
9-HOTrE	-1.23	-1.62	4.05	5.21	0.06	0.47	0.15	0.10
Avocadyne 4-acetate	-1.00	-1.15	-1.13	1.08	0.00	0.02	0.02	0.01
Glycerol-2-phosphate	1.51	1.13	na	na	0.30	0.04	na	na
Glycerol-3-phosphate	1.50	1.29	-2.50	-1.11	0.46	0.37	0.61	0.07
Glycerophosphocholine	3.97	na	-1.72	1.16	0.06	na	0.17	0.20
Linoleic acid	-1.62	-1.21	6.58*	-1.50	0.97	0.62	1.97	0.20
Linolenic acid	na	1.69	-3.98	-2.27	na	0.34	0.31	0.41
LPA (0:0/18:2(9Z,12Z))	9.82	-1.78	1.10	-1.26	0.95	0.90	0.05	0.26
LysoPC (16:0)	1.34	na	na	na	0.05	na	na	na
LysoPE (18:1)	na	na	5.20	6.76	na	na	0.42	0.52
Oleic acid	9.69	1.05	1.27	-1.21	0.31	0.03	0.20	0.10
Palmitic acid	6.38*	2.29	3.67	-4.96	0.24	0.31	0.10	0.12
Pantothenol	-5.81*	6.42	1.27	4.13	0.88	1.72	0.10	1.42
Nucleotides								
Adenine	1.46	3.89	-1.08	4.10	0.29	0.51	0.04	0.40
Adenosine	-2.44	-1.03	-1.58	-1.22	2.15	0.07	0.84	0.52
Cytosine	-1.26	-1.43	2.50	-1.51	0.12	0.31	0.27	0.12
Inosine	-4.68	na	na	na	0.17	na	na	na
Uridine	1.02	-1.06	-2.79*	-1.46	0.01	0.04	0.33	0.10
Cofactors								
Nicotinamide	-2.12	1.20	1.28	4.86	1.94	0.54	0.46	3.43

Metabolite name	FC[a]				VIP scores[b]			
	Shoot		Root		Shoot		Root	
	IR64	Pokkali	IR64	Pokkali	IR64	Pokkali	IR64	Pokkali
Nicotinate	-4.14	-1.29	4.07	1.68	0.52	0.19	0.61	0.55
Nicotinate ribonucleoside	-4.25	na	na	4.30	1.26	na	na	0.90
Pantothenic acid	1.52	-1.37	-1.40	-1.54	0.55	0.54	0.35	0.78
Pyridoxate	1.24	-4.02	-2.94	7.90	0.17	0.46	0.15	0.26
Pyridoxine	1.69	na	-1.48	-1.94	0.15	na	0.43	1.45
Flavonoids and Terpenoids								
Luteolin 7-O-glucoside	na	6.93	3.10	1.03	na	0.29	0.77	0.01
Medicarpin	2.28	5.10	2.13	1.25	0.29	0.54	0.14	0.05
(-)-Menthone	-3.96	-1.48	1.33	-15.31	0.10	0.06	0.37	1.49
Tricin 4'-O-(erythro-β-guaiacylglyceryl) ether	6.93	na	na	na	1.37	na	na	na
(1R,6R)-6-Hydroxy-2-succinylcyclohexa-2,4-diene-1-carboxylate	1.23	1.78	-1.04	1.78	0.05	0.27	0.00	0.06
4-Hydroxycinnamate	1.38	1.89	2.58	-1.88	2.80	3.31	0.29	0.30
6(E)-8-Oxogeraniol	-6.46*	-1.75	4.42	-1.05	5.20	1.44	0.89	0.04
Cafestol	na	4.71	na	na	na	0.06	na	na
Ferulate	-1.25	1.14	-1.86	-1.44	0.03	0.03	0.07	0.04
Fusicoplagin A	-7.58*	1.60	5.99*	-1.57	1.39	0.73	0.87	0.45
Momilactone A	-2.12	9.22	1.79	1.59	0.10	0.11	0.02	0.01
Phytocassane C	na	na	na	4.12	na	na	na	0.30
Pinoresinol	3.83	na	6.88*	7.22	0.06	na	0.08	0.12
Sinapic acid	2.39	1.56	-4.50	na	0.67	0.42	0.14	na
Syringin	-2.07	-1.23	-2.97	-1.01	0.19	0.05	0.77	0.01
Others								
1-O-Feruloyl-β-D-glucose	-1.50	1.43	-1.78	-1.80	0.19	0.19	0.05	0.10
(2R)-1-O-β-D galactopyranosylglycerol	-6.13	-6.58	2.04	12.27	0.46	0.29	0.15	0.47
2-Amino-1,3,4-tetradecanetriol	1.33	na	na	na	0.39	na	na	na
2'-Deoxyribose	1.61	-1.55	2.68	-2.10	0.09	0.13	0.28	0.22
2-Hydroxycyclohexan-1-one	1.46	-2.65	1.27	-3.21	0.77	1.79	0.62	6.49
2-Isopropylmaleate	1.45	1.12	1.83	2.02	0.07	0.01	0.13	0.16
2,6-Dihydroxy-N-methylmyosmine	1.02	-1.01	-3.79	1.82	0.01	0.00	0.51	0.46
4-Hydroxybenzoic acid	2.44	5.46	3.88	na	0.24	0.39	0.19	na
4-Methylumbelliferyl glucuronide	-3.81	-3.86	na	na	0.79	0.36	na	na
5-(3'-Carboxy-3'-oxopropenyl)-4,6-dihydroxypicolinate	na	-4.78	na	na	na	0.05	na	na
5,6 Dihydrothymine	2.31	1.44	-6.21*	-3.39	3.28	0.90	2.32	0.83
Diphosphoric acid	-1.83	-1.23	1.02	4.20	1.23	0.38	0.02	0.72
Dodecyl (dimethyl) amine oxide	-3.85	4.76	2.08	1.86	0.16	0.46	2.85	2.29
Methylbenzoate	-1.70	-1.24	1.81	-1.54	0.13	0.18	0.72	0.69
Trigonelline	1.70	-3.00	-1.32	-1.59	0.18	0.55	0.05	0.05

[a]FC means fold changed and calculated using formula Fe toxicity/control condition. [b]Variation in Projection (VIP) scores were calculated using Partial Least Square-Discriminant Analysis (PLS-DA).[c]na = Not available. The number followed by asterisks (*) means not significantly up- or down-accumulated based on the Student's T-test (α=0.05)

The most valuable metabolite based on Partial Least Square-Discriminant Analysis (PLS-DA) analysis were 6(E)-8-oxogeraniol (-6.46-fold; VIP score = 5.20) and ACC (2.33-fold; VIP score = 3.24) in shoot tissue of IR64 and Pokkali, respectively. The 5,6-dihydrothymine (-6.21-fold; VIP score = 2.32) in root tissue of IR64 and galactose (4.55-fold; VIP score = 0.65) in root tissue of Pokkali are showed most valuable metabolite based on PLS-DA analysis. These results suggested that both the primary- and secondary metabolites simultaneously regulated under Fe toxicity stress, especially carbohydrate, terpenoid, and other small-weight compounds.

Furthermore, the significantly altered metabolites involved in the primary and secondary metabolism, glycolysis, and TCA cycle were mapped in simplified biological pathway maps (Figures 5-6). As shown in Figure 5, some secondary metabolites were down-accumulated in shoot tissue of IR64 after exposure to Fe toxicity stress, such as 6(E)-8-Oxogeraniol

and Fusicoplagin A. Interestingly, most significantly metabolites in shoot tissue of IR64 showed down-accumulated in both glycolysis and TCA cycle, include: metabolite of the 3-P-glycerate-derived pathway, i.e., palmitic acid; and metabolite of the p-enolpyruvate (PEP)-derived pathway, i.e., 3-dehydroquinate; metabolite of the oxaloacetate-derived pathway, i.e., asparagine and aspartate; metabolite of the α-ketoglutaric acid-derived pathway, i.e., hydroxyproline. In shoot tissue of Pokkali, ACC, a metabolite of the oxaloacetate-derived pathway in TCA cycle and homovanillic acid, a metabolite of the p-enolpyruvate (PEP)-derived pathway in glycolysis process were up-accumulated after exposure to Fe toxicity stress.

At the same time, in the root tissues of Pokkali, most significantly metabolites were up-accumulated in glycolysis and TCA cycle after exposed to Fe toxicity stress (Figure 6). Two metabolites of the glucose-derived pathway, i.e., gluconate and galactose. Linoleic acid, a
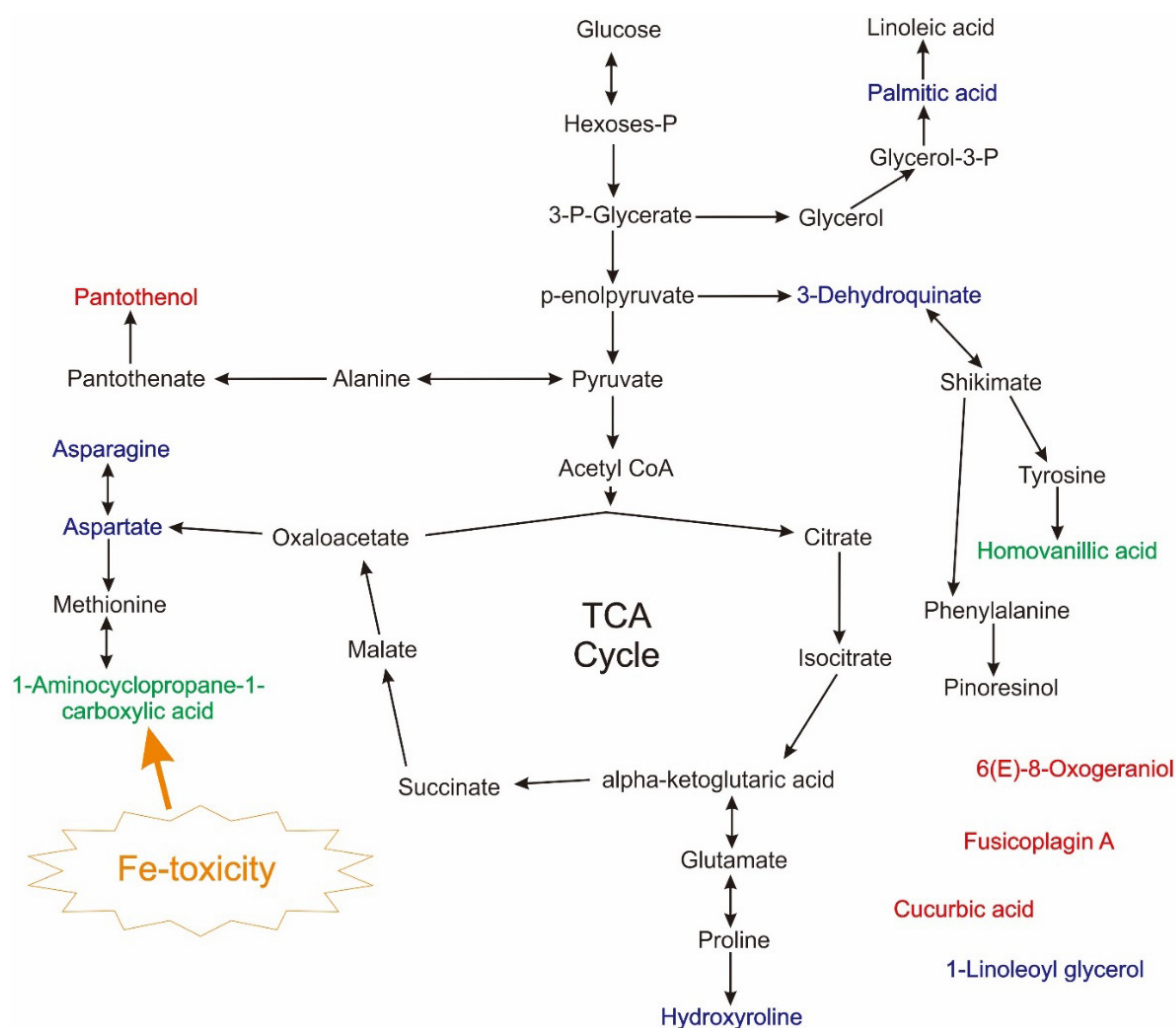
Red letters = down-accumulated in IR64; Blue letters = up-accumulated in IR64; Green letters = up-accumulated in Pokkali

FIGURE 5. Change in metabolites of the metabolic pathways in shoot tissue of rice after Fe toxicity stress
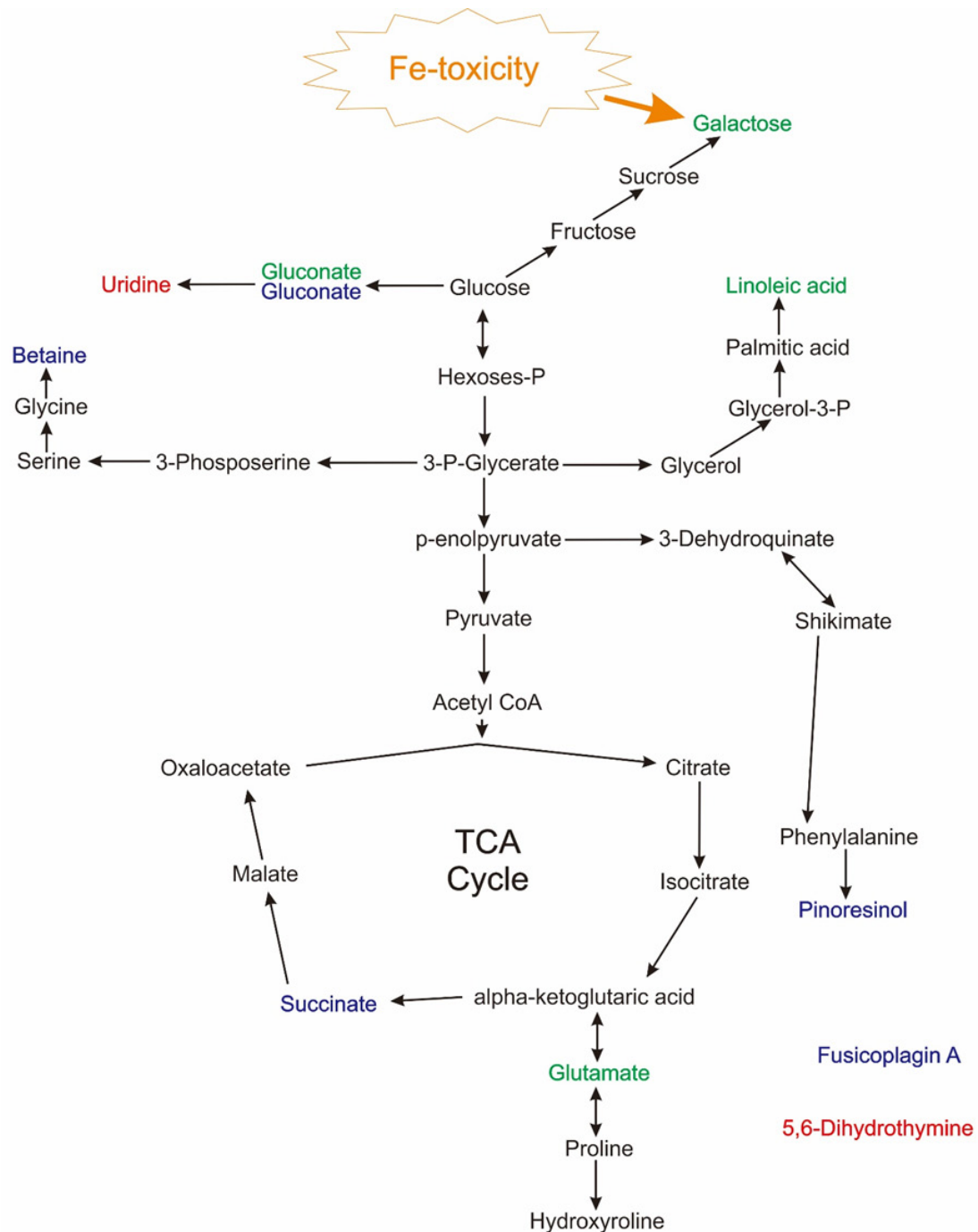
Red letters = down-accumulated in IR64; Blue letters = up-accumulated in IR64; Green letters = up-accumulated in Pokkali

FIGURE 6. Change in metabolites of the metabolic pathways in the root of rice tissue after
Fe toxicity stress

metabolite of the 3-P-glycerate-derived pathway and metabolite of the α-ketoglutaric acid-derived pathway in TCA cycle, i.e., glutamate also up-accumulated after exposure to Fe toxicity stress in root tissue of Pokkali.

After exposure to Fe toxicity stress, the significantly changed metabolites in shoot and root tissues were subjected to pathway analysis to know the meaningful involved metabolic pathways. The results showed that

alanine, aspartate, and glutamate metabolism; cyanoamino acid metabolism; aminoacyl-tRNA biosynthesis; cysteine and methionine metabolism; and monobactam biosynthesis in shoot tissues were significantly altered by Fe toxicity stress (Figure 7(A); Supplementary Table S2). In comparison, butanoate metabolism; alanine, aspartate, and glutamate metabolism; glyoxylate and dicarboxylate metabolism; and linoleic acid metabolism in root tissues were significantly altered by Fe toxicity stress (Figure 7(B); Supplementary Table S3).
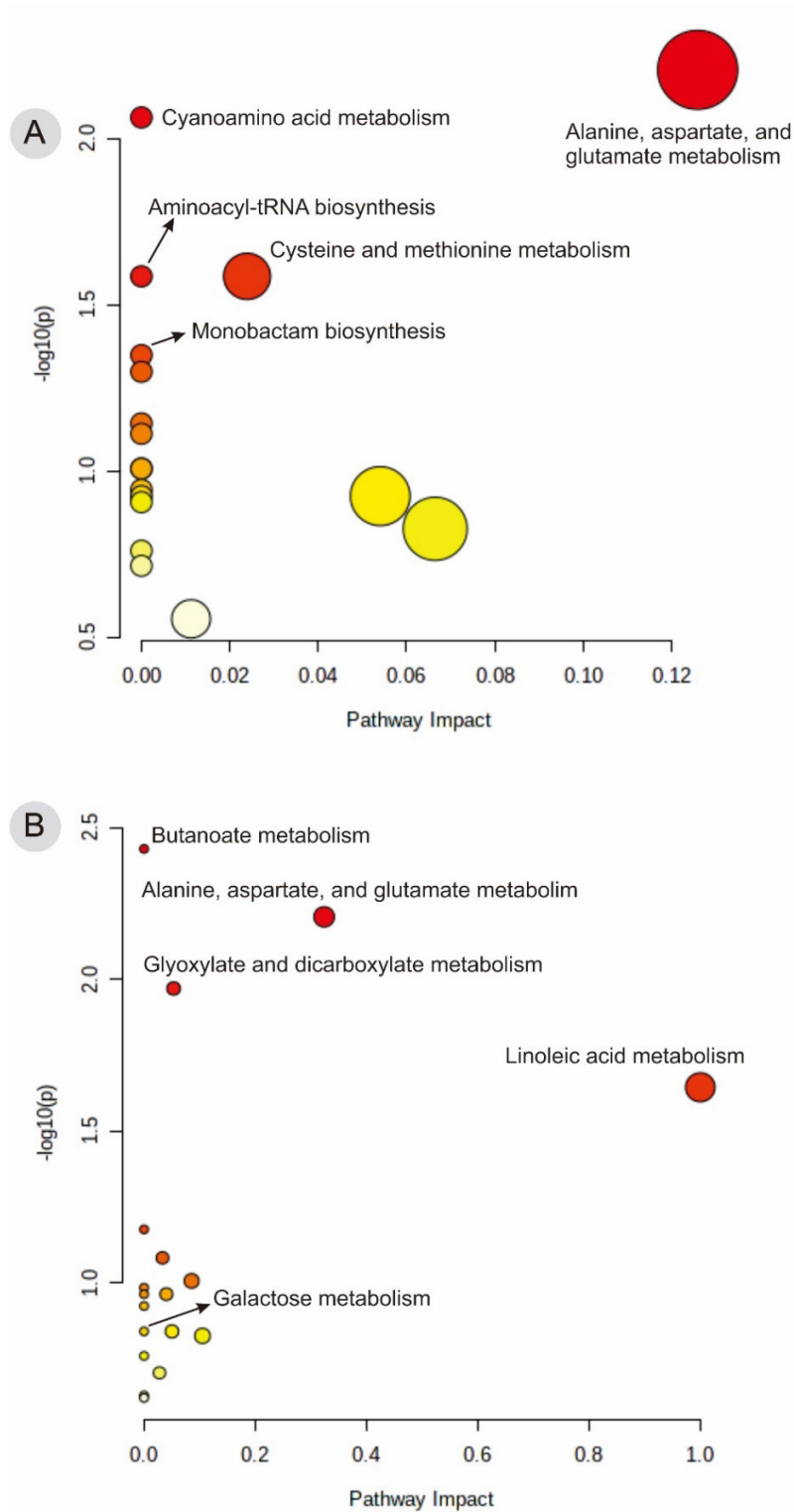

FIGURE 7. Plot summarizing the metabolic pathways in the shoot (A) and root (B) tissues of rice after Fe toxicity stress from pathway analysis

DISCUSSION

Fe toxicity is one of the common problems in agriculture, especially in swampy lands. Numerous scientific evidences have been reported that Fe toxicity in rice impaired growth, metabolism, to productivity. IR64 and Pokkali as two rice varieties with distinct tolerance level to Fe toxicity (Figure 1). As previously reported, IR64 is a sensitive rice variety, while Pokkali is a tolerant rice variety (Turhadi et al. 2019, 2018). Using UHPLC-Q-Orbitrap HRMS-based metabolite profiling combined with comprehensive statistical analyses, in this study, we investigated the metabolic characteristics of rice after exposure to Fe toxicity stress. A total of 102 primary and secondary metabolites were identified in this study (Figure 2(A)-2(B) & 4(B)-4(J)). This metabolite composition is reflected a metabolic regulation in rice after exposure to Fe toxicity stress. Moreover, there was a noticeable difference in metabolite composition between shoot and root tissues of rice (Figure 3 & 4(A)). This result suggested that shoot and root tissues have a different response after exposure to Fe toxicity stress.

Some glycolysis and TCA cycle intermediates were up-accumulated in IR64 after exposure to Fe toxicity stress. In contrast, Pokkali as tolerant rice variety to Fe toxicity stress showed that significantly up-accumulated in their metabolites, such as 1-aminocyclopropane-1-carboxylate (ACC) and homovanillic acid (Figure 5). These two metabolites exhibit as glycolysis and TCA cycle intermediates, respectively. As noted in this study, ACC strongly suggested as a critical metabolite in Pokkali to tolerate Fe toxicity stress in shoot tissues. This finding is supported by previous transcriptomic studies which reported Fe toxicity stress in rice affected ethylene biosynthesis genes-related (Aung et al. 2018; Stein et al. 2019). Gene involved in iron homeostasis, especially genes related to the methionine cycle, such as S-adenosyl-methionine synthetase 1 (*OsSAMS1* and *OsSAMS2*) were up-regulated in the shoot (stem, old leaf, and newest leaf) after exposure to Fe toxicity stress of 0.36-2.50 mM (Aung et al. 2018). Furthermore, a tolerant cultivar to Fe toxicity stress, EPAGRI 108 showed up-regulated genes involved in root cell wall biosynthesis and lignification (Stein et al. 2019). ACC content in shoot tissues of *Arabidopsis thaliana* was up-accumulated after exposure to Cadmium (Cd^{2+}) toxicity stress of 5 and 10 μM and was positively correlated with ethylene content (Schellingen et al. 2014). ACC is a direct precursor and regulator in the ethylene biosynthesis mechanism, which involves the ACC synthase (ACS) enzyme (Adams & Yang 1979; Vanderstraeten & Van Der Straeten 2017). ACC is reported as a direct precursor in ethylene production and as a signaling molecule for root-to-shoot communication. ACC will transport from root to shoot when the plant experienced stress (Yoon & Kieber 2013). ACC is also involved in regulating plant development, cell wall signaling, guard mother cell division, and pathogen virulence (Polko & Kieber 2019). Based on this study, ACC in the shoot of tolerant rice variety was suggested as a precursor in ethylene production pathway and as a signaling molecule in cell wall biosynthesis mechanism during Fe toxicity stress tolerance mechanism.

To maintain their life during Fe excess conditions, root tissues of rice also produce more galactose. As indicated in this study, rice var. Pokkali under Fe toxicity stress showed that significantly up-accumulated the galactose in root tissues under Fe toxicity stress (Table 1). This result similar to previous studies that galactose will increase during stress conditions (Gupta & De 2017; Wang et al. 2015). Galactose is increased in radish roots after exposure to the stress of 1000 mg L^{-1} $Pb(NO_3)_2$ for 72 h. It is suggested that photoassimilates were stored as hexoses after exposure to the stress to strengthen the glycolysis to cope the stress (Wang et al. 2015). A salt-tolerant rice variety var. Bhutnath also showed that salt stress induced the increase of galactose content (Gupta & De 2017). According to Yancey (2005), sugars act as osmoprotectants, help to maintain osmotic balance, stabilize macromolecules, provide an immediate energy source for plants to restart the growth. Furthermore, sugar synthesis is also reported as a favorable mechanism for improving ROS detoxification (Wu et al. 2014). Based on this study, galactose in the root of tolerant rice variety is suggested as an energy source to maintain their life during Fe toxicity stress.

CONCLUSIONS

Using UHPLC-Q-Orbitrap HRMS-based metabolomic obtained 102 metabolites in root and shoot tissues of rice. Comprehensive univariate and multivariate analysis in all identified primary and secondary metabolites suggested that 1-aminocyclopropane-1-carboxylate and galactose in shoot and root tissues as metabolite markers significantly up-accumulated in Fe toxicity tolerant rice var. Pokkali after exposure to Fe toxicity stress. The biological pathway related to 1-aminocyclopropane-1-carboxylate and galactose might be targeted for further study to explore tolerance mechanism to Fe toxicity stress in rice.

REFERENCES

Adams, D.O. & Yang, S.F. 1979. Ethylene biosynthesis: Identification of 1-aminocyclopropane-1-carboxylic acid as an intermediate in the conversion of methionine to ethylene. *Proc. Natl. Acad. Sci. USA* 76(1): 170-174.

Albano, J.P., Miller, W.B. & Halbrooks, M.C. 1996. Iron toxicity stress causes bronze speckle, a specific physiological disorder of marigold (*Tagetes erecta* L.). *J. Amer. Soc. Hort. Sci.* 121(3): 430-437.

Audebert, A. & Sahrawat, K.L. 2000. Mechanisms for iron toxicity tolerance in lowland rice. *J. Plant Nutr.* 23(11&12): 1877-1885.

Aung, M.S. & Masuda, H. 2020. How does rice defend against excess iron?: Physiological and molecular mechanisms. *Front. Plant. Sci.* 11: 1102.

Aung, M.S., Masuda, H., Kobayashi, T. & Nishizawa, N.K. 2018. Physiological and transcriptomic analysis of responses to different levels of iron excess stress in various rice tissues. *J. Soil Sci. Plant Nutr.* 64(3): 370-385.

Bashir, K., Hanada, K., Shimizu, M., Seki, M., Nakanishi, H. & Nishizawa, N.K. 2014. Transcriptomic analysis of rice in response to iron deficiency and excess. *Rice* 7(18): 1-15.

Begum, M.C., Islam, M.S., Islam, M., Amin, R., Parvez, M.S. & Kabir, A.H. 2016. Biochemical and molecular responses underlying differential arsenic tolerance in rice (*Oryza sativa* L.). *Plant Physiol. Biochem.* 104: 266-277.

Chang, Y., Zhao, C., Zhu, Z., Wu, Z., Zhou, J., Zhao, Y., Lu, X. & Xu, G. 2012. Metabolic profiling based on LC/MS to evaluate unintended effects of transgenic rice with *cry1Ac* and *sck* genes. *Plant Mol. Biol.* 78: 477-487.

De Dorlodot, S., Lutts, S. & Bertin, P. 2005. Effects of ferrous iron toxicity on the growth and mineral composition of an interspecific rice. *J. Plant Nutr.* 28: 1-20.

Do Amaral, M.N., Arge, L.W.P., Benitez, L.C., Danielowski, R., da Silveira, S.F., da Rosa Farias, D., de Oliveira, A.C., da Maia, L.C. & Braga, E.J.B. 2016. Comparative transcriptomics of rice plants under cold, iron, and salt stresses. *Funct. Integr. Genomics.* 16(5): 567-579.

Dong, X., Chen, W., Wang, W., Zhang, H., Liu, X. & Luo, J. 2014. Comprehensive profiling and natural variation of flavonoids in rice. *J. Integrative Plant Biol.* 56(9): 876-886.

Engel, K., Asch, F. & Becker, M. 2012. Classification of rice genotypes based on their mechanisms of adaptation to iron toxicity. *J. Plant Nutr. Soil. Sci.* 175: 871-881.

Finatto, T., de Oliveira, A.C., Chaparro, C., da Maia, L.C., Farias, D.R., Woyann, L.G., Mistura, C.C., Soares-Bresolin, A.P., Llauro, C., Panaud, O. & Picault, N. 2015. Abiotic stress and genome dynamics: Specific genes and transposable elements response to iron excess in rice. *Rice* 8(13): 1-18.

Gupta, P. & De, B. 2017. Metabolomics analysis of rice responses to salinity stress revealed elevation of serotonin, and gentisic acid levels in leaves of tolerant varieties. *Plant Signaling Behav.* 12(7): e1335845.

Hall, R.D. & Hardy, N.W. 2012. *Plant Metabolomics: Methods and Protocol.* New York: Humana Press.

Hill, C.B. & Roessner, U. 2013. Metabolic profiling of plants by GC-MS. In *The Handbook of Plant Metabolomics*, edited by Weckwerth, W. & Kahl, G. Weinheim: Wiley-VCH Verlag GmBH & Co.

Hu, C., Shi, J., Quan, S., Cui, B., Kleessen, S., Nikoloski, Z., Tohge, T., Alexander, D., Guo, L., Lin, H., Wang, J., Cui, X., Rao, J., Luo, Q., Zhao, X., Fernie, A.R. & Zhang, D. 2014. Metabolic variation between japonica and indica rice cultivars as revealed by non-targeted metabolomics. *Sci. Rep.* 4: 5067.

Hu, C., Tohge, T., Chan, S.A., Song, Y., Rao, J., Cui, B., Lin, H., Wang, L., Fernie, A.R., Zhang, D. & Shi, J. 2016. Identification of conserved and diverse metabolic shifts during rice grain development. *Sci. Rep.* 6: 20942.

Jorge, T.F., Rodrigues, J.A., Caldana, C., Schmidt, R., van Dongen, J.T., Thomas-Oates, J. & Antonio, C. 2016. Mass spectrometry-based plant metabolomics: Metabolite response to abiotic stress. *Mass Spec. Rev.* 35: 620-649.

Jung, E.S., Lee, S., Lim, S.H., Ha, S.H., Liu, K.H. & Lee, C.H. 2013. Metabolite profiling of the short-term responses of rice leaves (*Oryza sativa* cv. Ilmi) cultivated under different LED lights and its correlations with antioxidant activities. *Plant Sci.* 210: 61-69.

Kabir, A.H., Begum, M.C., Haque, A., Amin, R., Swaraz, A.M., Haider, S.A., Paul, N.K. & Hossain, M.M. 2016. Genetic variation in Fe toxicity tolerance is associated with the regulation of translocation and chelation of iron along with antioxidant defence in shoots of rice. *Funct. Plant Biol.* 43(11): 1070-1081.

Khabaz-Saberi, H., Rengel, Z., Wilson, R. & Setter, T.L. 2010. Variation for tolerance to high concentration of ferrous iron (Fe^{2+}) in Australian hexaploid wheat. *Euphytica* 172(2): 275-283.

Kovačević, V., Vukadinović, V. & Bertić, B. 1988. Excessive iron and aluminum uptake and nutritional stress in corn (*Zea mays* L.) plants. *J. Plant Nutr.* 11(6-11): 1263-1272.

Kusano, M., Yang, Z., Okazaki, Y., Nakabayashi, R., Fukushima, A. & Saito, K. 2015. Using metabolomic approaches to explore chemical diversity in rice. *Mol. Plant.* 8: 58-67.

Lim, D.K., Mo, C., Lee, J.H., Long, N.P., Dong, Z., Li, J., Lim, J. & Kwon, S.W. 2018a. The integration of multi-platform MS-based metabolomics and multivariate analysis for the geographical origin discrimination of *Oryza sativa* L. *J. Food Drug Anal.* 26: 769-777.

Lim, D.K., Long, N.P., Mo, C., Dong, Z., Lim, J. & Kwon, S.W. 2018b. Optimized mass spectrometry-based metabolite extraction and analysis for the geographical discrimination of white rice (*Oryza sativa* L.): A method comparison study. *J. AOAC Intern.* 101(2): 498-506.

Lucassen, E.C.H.E.T., Smolders, A.J.P. & Roelofs, J.G.M. 2000. Increased groundwater levels cause iron toxicity in *Glyceria fluitans* (L.). *Aquatic Bot.* 66: 321-327.

Mahender, A., Swamy, B.P.M., Anandan, A. & Ali, J. 2019. Tolerance of iron deficient and -toxic soil conditions in rice. *Plants* 8: 31.

Navarro-Reig, M., Jaumot, J., Piña, B., Moyano, E., Galceran, M.T. & Tauler, R. 2017. Metabolomic analysis of the effects of cadmium and copper treatment in *Oryza sativa* L. using untargeted liquid chromatography coupled to high resolution mass spectrometry and all-ion fragmentation. *Metallomics* 9(6): 660-675.

Navarro-Reig, M., Jaumot, J., García-Reiriz, A. & Tauler, R. 2015. Evaluation of changes induced in rice metabolome by Cd and Cu exposure using LC-MS with XCMS and MCR-ALS data analysis strategies. *Anal. Bioanal. Chem.* 407: 8835-8847.

Nugraha, Y., Ardie, S.W., Ghulamahdi, M., Suwarno & Aswidinnoor, H. 2015. Nutrient culture media with agar is effective for early and rapid screening of iron toxicity tolerance in rice. *J. Crop Sci. Biotech.* 19(1): 61-70.

Obata, T. & Fernie, A.R. 2012. The use of metabolomics to dissect plant responses to abiotic stresses. *Cell Mol. Life Sci.* 69: 3225-3243.

Oh, M., Park, S., Kim, H., Choi, G.J. & Kim, S.H. 2021. Application of UPLC-QTOF-MS based untargeted metabolomics in identification of metabolites induced in pathogen-infected rice. *Plants (Basel)* 10(2): 213.

Polko, J.K. & Kieber, J.J. 2019. 1-Aminocyclopropane 1-carboxylic acid and its emerging role as an ethylene independent growth regulator. *Front. Plant Sci.* 10: 1602.

Quinet, M., Vromman, D., Clippe, A., Bertin, P., Lequeux, H., Dufey, I., Lutts, S. & Lefèvre, I. 2012. Combined transcriptomic and physiological approaches reveal strong differences between short- and long-term response of rice (*Oryza sativa*) to iron toxicity. *Plant Cell Environ.* 35(10): 1837-1859.

Sangwan, N.S., Tiwari, P., Mishra, S.K., Yadav, R.K., Tripathi, S., Kushwaha, A.K. & Sangwan, R.S. 2015. Plant metabolomics: An overview of technology platforms for applications in metabolism. In *PlantOmics: The Omics of Plant Science*, edited by Barh, D., Khan, M. & Davies, E. New Delhi: Springer.

Schellingen, K., Van Der Straeten, D., Vandenbussche, F., Prinsen, E., Remans, T., Vangronsveld, J. & Cuypers, A. 2014. Cadmium-induced ethylene production and responses in *Arabidopsis thaliana* rely on *ACS2* and *ACS6* gene expression. *BMC Plant Biol.* 14: 214.

Snowden, R.E.D. & Wheeler, B.D. 1993. Iron toxicity to fen plant species. *J. Ecol.* 81: 35-46.

Stein, R.J., Duarte, G.L., Scheunemann, L., Spohr, M.G., de Araújo Júnior, A.T., Ricachenevsky, F.K., Rosa, L.M.G., Zanchin, N.I.T., Santos, R.P. & Fett, J.P. 2019. Genotype variation in rice (*Oryza sativa* L.) tolerance to Fe toxicity might be linked to root cell wall lignification. *Front. Plant Sci.* 10: 746.

Turhadi, Miftahudin, Hamim & Ghulamahdi, M. 2021. The effectiveness of nutrient culture solutions with agar addition as an evaluation media of rice under iron toxicity conditions. *Bioeduscience* 5(1): 24-29.

Turhadi, T., Hamim, H., Ghulamahdi, M. & Miftahudin, M. 2019. Iron toxicity-induced physiological and metabolite profile variations among tolerant and sensitive rice varieties. *Plant Signal Behav.* 14(12): 1682829.

Turhadi, T., Hamim, H., Ghulamahdi, M. & Miftahudin, M. 2018. Morpho-physiological responses of rice genotypes and its clustering under hydroponic Fe toxicity conditions. *Asian J. Agri. Biol.* 6(4): 495-505.

Vanderstraeten, L. & Van Der Straeten, D. 2017. Accumulation and transport of 1-aminocyclopropane-1-carboxylic acid (ACC) in plants: Current status, considerations for future research and agronomic applications. *Front. Plant Sci.* 8: 38.

Wang, Y., Xu, L., Shen, H., Wang, J., Liu, W., Zhu, X., Wang, R., Sun, X. & Liu, L. 2015. Metabolomic analysis with GC-MS to reveal potential metabolites and biological pathways involved in Pb & Cd stress response of radish roots. *Sci. Rep.* 5: 18296.

Widodo, Patterson, J.H., Newbigin, E., Tester, M., Bacic, A. & Roessner, U. 2009. Metabolic responses to salt stress of barley (*Hordeum vulgare* L.) cultivars, Sahara and Clipper, which differ in salinity tolerance. *J. Exp. Bot.* 60(14): 4089-4103.

Wu, L.B., Shhadi, M.Y., Gregorio, G., Matthus, E., Becker, M. & Frei, M. 2014. Genetic and physiological analysis of tolerance to acute iron toxicity in rice. *Rice* 7(1): 8.

Wu, L.B, Ueda, Y., Lai, S.K. & Frei, M. 2016. Shoot tolerance mechanisms to iron toxicity in rice (*Oryza sativa* L.). *Plant Cell Environ.* 40(4): 570-584.

Xia, J. & Wishart, D.S. 2016. Using metaboAnalyst 3.0 for comprehensive metabolomics data analysis. *Curr. Protoc. Bioinformatics* 55: 14.10.1-14.10.91.

Xiao, R., Ma, Y., Zhang, D. & Qian, L. 2018. Discrimination of conventional and organic rice using untargeted LC-MS based metabolomics. *J. Cereal Sci.* 82: 73-81.

Yancey, P.H. 2005. Organic osmolytes as compatible, metabolic and counteracting cytoprotectants in high osmolarity and other stresses. *J. Exp. Biol.* 208(15): 2819-2830.

Yoon, G.M. & Kieber, J.J. 2013. 1-Aminocyclopropane-1-carboxylic acid as a signalling molecule in plants. *AoB PLANTS* 5: plt017.

Yoshida, S., Forno, D.A., Cock, J.H. & Gomez, K.A. 1976. *Laboratory Manual for Physiological Studies of Rice*. Manila: The International Rice Research Institute.

*Corresponding author; email: miftahudin@apps.ipb.ac.id

SUPPLEMENTARY TABLE 1

MW (g/mol)	RT (min)	Metabolite	Class
160.06	2.01	2-Aminoadipate	Amino acids & amino acid related
118.05	6.03	Allo-threonine	Amino acids & amino acid related
116.03	1.41	Betaine	Amino acids & amino acid related
144.07	7.14	Gamma-Guanidinobutyrate	Amino acids & amino acid related
140.03	2.30	Histidinol	Amino acids & amino acid related
161.04	2.14	Hydroxylysine	Amino acids & amino acid related
130.06	0.57	Hydroxyproline	Amino acids & amino acid related
188.09	20.83	Kynurenate	Amino acids & amino acid related
227.13	1.02	Leucylproline	Amino acids & amino acid related
142.05	1.51	Stacydrine	Amino acids & amino acid related
173.04	1.73	Arginine	Amino acids & amino acid related
131.04	0.15	Asparagine	Amino acids & amino acid related
132.07	2.95	Aspartate	Amino acids & amino acid related
146.04	0.72	Glutamate	Amino acids & amino acid related
154.05	0.75	Histidine	Amino acids & amino acid related
148.06	21.73	Methionine	Amino acids & amino acid related
164.07	0.73	Phenylalanine	Amino acids & amino acid related
114.03	2.39	Proline	Amino acids & amino acid related
104.04	3.60	Serine	Amino acids & amino acid related
203.09	3.37	Tryptophan	Amino acids & amino acid related
180.07	24.21	Tyrosine	Amino acids & amino acid related
149.00	1.83	beta-D-xylopyranose	Carbohydrate & Lipids
179.07	2.93	Galactose	Carbohydrate & Lipids
178.04	0.52	Glucosamine	Carbohydrate & Lipids
503.39	15.92	Melezitose	Carbohydrate & Lipids
341.24	16.13	Sucrose	Carbohydrate & Lipids
121.04	1.33	Nicotinamide	Cofactors
122.07	5.58	Nicotinate	Cofactors
254.88	22.85	Nicotinate ribonucleoside	Cofactors
218.03	1.36	Pantothenic acid	Cofactors
182.01	19.01	Pyridoxate	Cofactors
168.08	9.24	Pyridoxine	Cofactors
447.35	16.74	Luteolin 7-O-glucoside	Flavonoids & Terpenoids
269.21	17.89	Medicarpin	Flavonoids & Terpenoids
525.38	16.26	Tricin 4'-O-(erythro-β-guaiacylglyceryl) ether	Flavonoids & Terpenoids
295.23	17.19	13-HODE	Carbohydrate & Lipids
327.18	16.57	2,3-Dinor-8-isoprostaglandin F1alpha	Carbohydrate & Lipids
100.04	24.74	1-Aminocyclopropane-1-carboxylate	Carbohydrate & Lipids
353.27	16.40	1-Linoleoyl glycerol	Carbohydrate & Lipids
293.18	24.67	9-HOTrE	Carbohydrate & Lipids
325.10	17.42	Avocadyne 4-acetate	Carbohydrate & Lipids
169.09	10.04	Glycerol-2-Phosphate	Carbohydrate & Lipids
171.10	6.33	Glycerol-3-Phosphate	Carbohydrate & Lipids
257.18	15.81	Glycerophosphocholine	Carbohydrate & Lipids
279.16	10.33	Linoleic acid	Carbohydrate & Lipids

277.10	5.59	Linolenic acid	Carbohydrate & Lipids
433.33	15.41	LPA(0:0/18:2(9Z,12Z))	Carbohydrate & Lipids
483.27	14.88	LysoPC(16:0)	Carbohydrate & Lipids
478.29	12.91	LysoPE(18:1)	Carbohydrate & Lipids
281.25	16.06	Oleic acid	Carbohydrate & Lipids
255.12	0.30	Palmitic acid	Carbohydrate & Lipids
204.02	5.45	Pantothenol	Carbohydrate & Lipids
134.04	24.78	Adenine	Nucleotides
266.15	15.23	Adenosine	Nucleotides
110.02	13.43	Cytosine	Nucleotides
267.16	8.97	Inosine	Nucleotides
243.16	10.02	Uridine	Nucleotides
145.09	7.41	2-Oxoglutarate	Organic acids
189.04	1.86	3-Dehydroquinate	Organic acids
88.04	5.26	3-Hydroxypropionate	Organic acids
367.28	16.00	3-O-Feruloylquinic acid	Organic acids
183.90	17.15	3-Phosphoserine	Organic acids
199.10	5.42	4-Fumaryl-acetoacetate	Organic acids
103.04	13.83	4-Hydroxybutyric acid	Organic acids
128.05	23.71	5-Oxoproline	Organic acids
215.09	0.49	6-Aminopenicillanate	Organic acids
175.06	0.21	Ascorbic acid	Organic acids
186.96	0.59	Azelaic Acid	Organic acids
211.10	2.72	Cucurbic acid	Organic acids
105.02	17.94	Glycerate	Organic acids
195.07	4.07	Gluconic Acid	Organic acids
181.09	0.84	Homovanillic acid	Organic acids
287.22	14.69	Ophthalmate	Organic acids
151.04	3.24	Phenoxyacetic acid	Organic acids
117.05	5.99	Succinate	Organic acids
191.11	14.37	2,6-Dihydroxy-N-methylmyosmine	Others
253.14	0.08	(2R)-1-O-beta-D galactopyranosylglycerol	Others
355.32	16.05	1-O-Feruloyl-β-D-glucose	Others
260.08	5.94	2-Amino-1,3,4-tetradecanetriol	Others
133.05	1.01	2'-Deoxyribose	Others
113.06	5.71	2-Hydroxycyclohexan-1-one	Others
157.06	0.63	2-Isopropylmaleate	Others
137.07	6.63	4-Hydroxybenzoic acid	Others
351.18	10.23	4-Methylumbelliferyl glucuronide	Others
252.10	20.17	5-(3'-Carboxy-3'-oxopropenyl)-4,6-dihydroxypicolinate	Others
127.08	0.71	5,6 Dihydrothymine	Others
177.05	4.13	Diphosphoric acid	Others
228.16	16.05	Dodecyl (dimethyl) amine oxide	Others
135.07	19.74	Methylbenzoate	Others
136.04	0.92	Trigonelline	Others
153.07	0.42	(-)-Menthone	Flavonoids & Terpenoids

		(1R,6R)-6-Hydroxy-2-succinylcyclohexa-2,4-diene-1-carboxylate	
239.13	14.82		Flavonoids & Terpenoids
163.06	1.33	4-Hydroxycinnamate	Flavonoids & Terpenoids
167.07	2.51	6(E)-8-Oxo geraniol	Flavonoids & Terpenoids
315.25	17.07	Cafestol	Flavonoids & Terpenoids
193.05	4.45	Ferulate	Flavonoids & Terpenoids
438.04	1.35	Fusicoplagin A	Flavonoids & Terpenoids
313.17	21.55	Momilactone A	Flavonoids & Terpenoids
317.21	11.81	Phytocassane C	Flavonoids & Terpenoids
357.15	18.47	Pinoresinol	Flavonoids & Terpenoids
223.13	0.73	Sinapic acid	Flavonoids & Terpenoids
371.31	16.37	Syringin	Flavonoids & Terpenoids

SUPPLEMENTARY TABLE 2

Pathway	Total	Expected	Hits	Raw p	=-LOG10(p)	Holm adjust	FDR	Impact
Alanine, aspartate and glutamate metabolism	22	0.12545	2	0.0062104	2.2069	0.58999	0.4103	0.1259
Cyanoamino acid metabolism	26	0.14825	2	0.0086378	2.0636	0.81196	0.4103	0
Aminoacyl-tRNA biosynthesis	46	0.2623	2	0.025971	1.5855	1	0.61681	0
Cysteine and methionine metabolism	46	0.2623	2	0.025971	1.5855	1	0.61681	0.02392
Monobactam biosynthesis	8	0.045617	1	0.044826	1.3485	1	0.79648	0
Lysine biosynthesis	9	0.051319	1	0.050304	1.2984	1	0.79648	0
Nicotinate and nicotinamide metabolism	13	0.074127	1	0.071941	1.143	1	0.84249	0
Cutin, suberine and wax biosynthesis	14	0.079829	1	0.077282	1.1119	1	0.84249	0
Arginine biosynthesis	18	0.10264	1	0.09838	1.0071	1	0.84249	0
beta-Alanine metabolism	18	0.10264	1	0.09838	1.0071	1	0.84249	0
Carbon fixation in photosynthetic organisms	21	0.11974	1	0.11392	0.94338	1	0.84249	0
Biosynthesis of unsaturated fatty acids	22	0.12545	1	0.11905	0.92426	1	0.84249	0
Phenylalanine, tyrosine and tryptophan biosynthesis	22	0.12545	1	0.11905	0.92426	1	0.84249	0.05405
Fatty acid elongation	23	0.13115	1	0.12416	0.90603	1	0.84249	0
Arginine and proline metabolism	28	0.15966	1	0.14929	0.82598	1	0.94548	0.06649
Glycine, serine and threonine metabolism	33	0.18817	1	0.17378	0.75999	1	1	0
Fatty acid degradation	37	0.21098	1	0.19293	0.71459	1	1	0
Fatty acid biosynthesis	56	0.31932	1	0.2787	0.55487	1	1	0.01123

SUPPLEMENTARY TABLE 3

Pathway	Total	Expected	Hits	Raw p	=-LOG10(p)	Holm adjust	FDR	Impact
Butanoate metabolism	17	0.09694	2	0.00371	2.4307	0.35237	0.29499	0
Alanine, aspartate and glutamate metabolism	22	0.12545	2	0.00621	2.2069	0.58378	0.29499	0.32374
Glyoxylate and dicarboxylate metabolism	29	0.16536	2	0.0107	1.9707	0.99492	0.33877	0.0531
Linoleic acid metabolism	4	0.02281	1	0.02264	1.6452	1	0.53765	1
Nitrogen metabolism	12	0.06843	1	0.06657	1.1767	1	1	0
Sulfur metabolism	15	0.08553	1	0.0826	1.083	1	1	0.03315
Arginine biosynthesis	18	0.10264	1	0.09838	1.0071	1	1	0.08544
Pentose phosphate pathway	19	0.10834	1	0.10359	0.98469	1	1	0
Propanoate metabolism	20	0.11404	1	0.10877	0.96349	1	1	0
Citrate cycle (TCA cycle)	20	0.11404	1	0.10877	0.96349	1	1	0.0401
Biosynthesis of unsaturated fatty acids	22	0.12545	1	0.11905	0.92426	1	1	0
Galactose metabolism	27	0.15396	1	0.14431	0.8407	1	1	0
Glutathione metabolism	27	0.15396	1	0.14431	0.8407	1	1	0.05016
Arginine and proline metabolism	28	0.15966	1	0.14929	0.82598	1	1	0.10499
Glycine, serine and threonine metabolism	33	0.18817	1	0.17378	0.75999	1	1	0
Pyrimidine metabolism	38	0.21668	1	0.19766	0.70408	1	1	0.02773
Aminoacyl-tRNA biosynthesis	46	0.2623	1	0.23461	0.62965	1	1	0
Porphyrin and chlorophyll metabolism	47	0.268	1	0.23912	0.62138	1	1	0